

Complexes of Bis(chlorodimethylstannyl)- and Bis(dichloromethylstannyl)methanes with Aromatic Nitrogen Heterocycles

Martin Austin, Kassu Gebreyes, Henry G. Kuivila,* Kamal Swami, and Jon A. Zubieta*

Department of Chemistry, State University of New York at Albany Albany, New York 12222

Received July 28, 1986

The preparations and structures determined by X-ray diffraction of the following complexes of bis(chlorodimethylstannyl)methane and bis(dichloromethylstannyl)methane with aromatic nitrogen heterocycles are described: $\text{CH}_2(\text{ClMe}_2\text{Sn})_2\text{-C}_5\text{H}_5\text{N}$ (1) ($\text{C}_5\text{H}_4\text{N}$ = pyridine); $\text{CH}_2(\text{ClMe}_2\text{Sn})_2\text{-C}_4\text{H}_4\text{N}_2$ (2) ($\text{C}_4\text{H}_4\text{N}_2$ = pyridazine); $\text{CH}_2(\text{Cl}_2\text{MeSn})_2\text{-2C}_4\text{H}_4\text{N}_2$ (3) ($\text{C}_4\text{H}_4\text{N}_2$ = pyridazine); $\text{CH}_2(\text{ClMe}_2\text{Sn})_2\text{-2C}_3\text{H}_4\text{N}_2$ (4) ($\text{C}_3\text{H}_4\text{N}_2$ = pyrazole); $\text{CH}_2(\text{ClMe}_2\text{Sn})_2\text{-C}_4\text{H}_4\text{N}_2$ (5) ($\text{C}_4\text{H}_4\text{N}_2$ = pyrazine); $\text{CH}_2(\text{Cl}_2\text{MeSn})_2\text{-C}_4\text{H}_4\text{N}_2$ (6) ($\text{C}_4\text{H}_4\text{N}_2$ = pyrazine); $\text{CH}_2(\text{Cl}_2\text{MeSn})_2\text{-bpy}$ (7) (bpy = bipyridyl). Crystal data are as follows. 1: triclinic $P1$, $a = 7.192$ (2) Å, $b = 10.175$ (2) Å, $c = 12.853$ (3) Å, $\alpha = 111.76$ (1)°, $\beta = 95.09$ (1)°, $\gamma = 105.40$ (1)°, $V = 823.5$ (8) Å³, $D(\text{calcd}) = 1.86$ g cm⁻³ for $Z = 2$; $R = 0.037$ for 1691 reflections. 2: monoclinic $P2_1/n$, $a = 9.330$ (2) Å, $b = 17.224$ (3) Å, $c = 9.860$ (2) Å, $\beta = 97.78$ (1)°, $V = 1569.9$ (9) Å³, $D(\text{calcd}) = 1.96$ g cm⁻³ for $Z = 4$; $R = 0.036$ for 1865 reflections. 3: orthorhombic $Pnam$, $a = 8.758$ (2) Å, $b = 13.111$ (3) Å, $c = 16.366$ (3) Å, $V = 1879.2$ (9) Å³, $D(\text{calcd}) = 2.06$ g cm⁻³ for $Z = 4$; $R = 0.026$ for 815 reflections. 4: orthorhombic $P2_12_1$, $a = 10.178$ (2) Å, $b = 10.365$ (2) Å, $c = 17.670$ (3) Å, $V = 1864.0$ (8) Å³, $D(\text{calcd}) = 1.84$ g cm⁻³ for $Z = 4$; $R = 0.046$ for 1195 reflections. 5: triclinic $P1$, $a = 6.939$ (2) Å, $b = 9.624$ (2) Å, $c = 10.460$ (2) Å, $\alpha = 102.21$ (1)°, $\beta = 92.38$ (1)°, $\gamma = 90.39$ (1)°, $D(\text{calcd}) = 2.03$ g cm⁻³ for $Z = 1$; $R = 0.026$ for 1518 reflections. 6: orthorhombic space group $Pbnb$, $a = 9.964$ (2) Å, $b = 12.414$ (3) Å, $c = 12.510$ (3) Å, $V = 1547.3$ (9) Å³, $D(\text{calcd}) = 2.04$ g cm⁻³ for $Z = 4$; $R = 0.022$ for 860 reflections. 7: monoclinic $P2_1/n$, $a = 12.845$ (3) Å, $b = 11.617$ (2) Å, $c = 15.361$ (3) Å, $\beta = 95.45$ (1)°, $V = 2281.8$ (10) Å³, $D(\text{calcd}) = 1.69$ g cm⁻³ for $Z = 4$; $R = 0.051$ for 1344 reflections. The X...Sn...Y distances for both trigonal-bipyramidal and octahedral structures at tin fit the bond order correlation functions of Britton and Dunitz for $\text{S}_\text{N}2$ and $\text{S}_\text{N}3$ reaction pathways.

The preparation of a large number of complexes of organotin halides and analogous organotin Lewis acids with nitrogen ligands including heterocycles has been reported in the literature. Structures of some have been determined by single-crystal X-ray diffraction. Examples relevant to this report include those of pyridine with trimethyltin chloride¹ and of diethyltin dichloride with 2,2'-bipyridyl.² Our interest in the complexation behavior of bis(halostannyl)methanes and the novel structures formed with dimethyl sulfoxide^{3,4} prompted us to extend these studies to nitrogen heterocycles. In addition to the simple monofunctional pyridine we were particularly interested in the interactions of the bifunctional bis(halostannyl)methanes with the bifunctional donors pyrazole, pyrazine, pyridazine, and 2,2'-bipyridyl because these offered possibilities of forming complexes with varied structures. These expectations were realized.

Preparations

Preparations of the complexes were usually attempted with different stoichiometries in order to determine if more than one kind of complex crystallized with a particular donor. The compounds discussed below were the only ones that were isolated. Compositions were established by elemental analysis.

The preparation of the complex of pyridine with bis(chlorodimethylstannyl)methane yielded product 1 with

a 1:1 ratio of reactants. Even when a large excess of pyridine was used, this was the only complex isolated. In order to determine whether other complexes were formed but were much more soluble than this one, an NMR study of the system was conducted. Increments of pyridine were added to a solution of bis(chlorodimethylstannyl)methane and the values of $^2J(^{119}\text{Sn}-^1\text{H})$ determined in the proton spectra for both the methyl and methylene protons. As shown by the data plotted in Figure 1, the values of these parameters changed until the ratio of reactants was 1:1 and then leveled off with increasing pyridine concentration. Thus, no evidence for the formation of other complexes is provided by these results. As our primary interest was in the structures of the solid complexes, similar detailed studies were not made with the other donor ligands. Also the structure of the pyridine complex as determined by X-ray crystallography (see below) suggests why the 1:1 complex is quite stable.

Solid-State Structures

Atomic positional and thermal parameters for the methylene-bridged species 1 through 7 are collected in Tables XVIII to XXIV, respectively. Bond lengths and selected bond angles are presented in Tables IV-XVII. The structures are illustrated in Figures 2-8.

The structure of the pyridine derivative $[(\text{CH}_3)_2\text{ClSn}(\text{CH}_2)\text{SnCl}(\text{CH}_3)(\text{py})]$ (1) represents the prototype structure for adduct formation between methylene-bridged haloorganotin units and a nitrogen donor ligand. The structure consists of a discrete binuclear tin compound with the tin centers bridged by a methylene group, C(6). To a first approximation Sn(1) displays pyramidal geometry, with three carbon atoms Me(1), Me(2), and C(6) generating the basal plane and Cl(1) in the apical position. However, in common with many triorganotin halide structures, the tin coordination is expanded through a long

(1) (a) Beattie, I. R.; McQuillan, G. P.; Hulme, R. *Chem. Ind. (London)* 1962, 14219. (b) Hulme, R. *J. Chem. Soc.* 1963, 1524.

(2) Chadha, S. L.; Harrison, P. G.; Molloy, K. C. *J. Organomet. Chem.* 1980, 202, 247.

(3) Karol, T. J.; Hutchinson, J. P.; Hyde, J. R.; Kuivila, H. G.; Zubieta, J. A. *Organometallics* 1983, 2, 106.

(4) For HMPA complexes of phenyl analogues see: Geilen, M.; Jurkschat, K.; Meunier, J.; van Meerssche, M.; Piret, J. *Bull. Soc. Chim. Belg.* 1984, 93, 379.

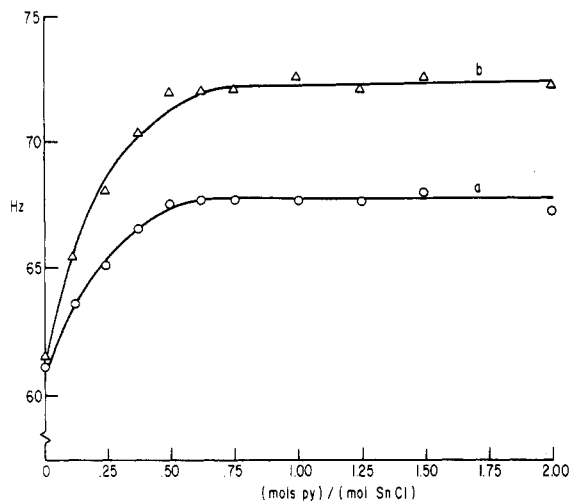


Figure 1. Effect of pyridine on $^{119}\text{Sn}-^1\text{H}$ coupling constants: a, $^2J(^{119}\text{Sn}-\text{CH}_3)$; b, $^2J(^{119}\text{Sn}-\text{CH}_2)$ in methylene chloride.

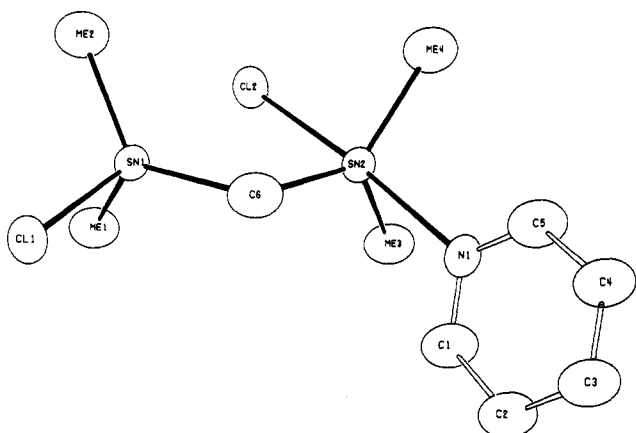


Figure 2. ORTEP view of the structure of $[(\text{CH}_3)_2\text{ClSn}(\text{CH}_2)\text{Sn}(\text{NC}_5\text{H}_5)\text{Cl}(\text{CH}_3)_2]$ (1).

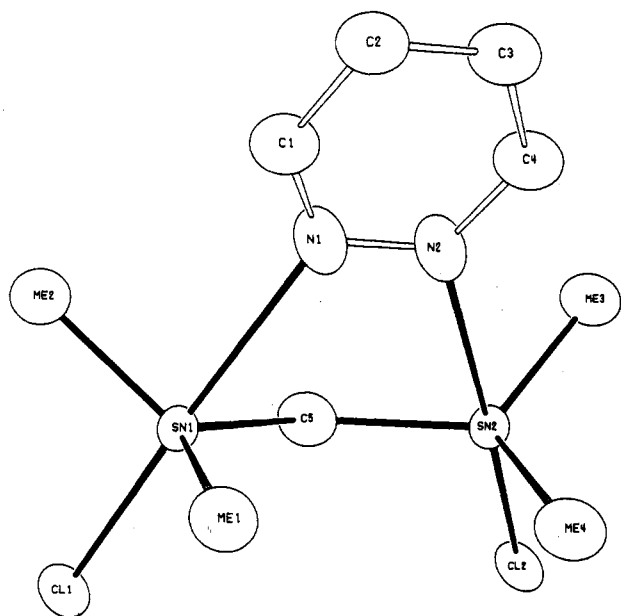


Figure 3. ORTEP view of the structure of $[(\text{CH}_3)_2\text{ClSn}(\text{C}-\text{H}_2)(\text{N}_2\text{C}_4\text{H}_4)\text{SnCl}(\text{CH}_3)_2]$ (2).

interaction, 3.009 (3) Å, to Cl(2), which is directly bonded to Sn(2). The coordination at Sn(1) may thus be described as trigonal-bipyramidal with Me(1), Me(2), and C(6) in the equatorial plane and Cl(1) and Cl(2) in the axial positions, a pattern consistent with the general rule that more

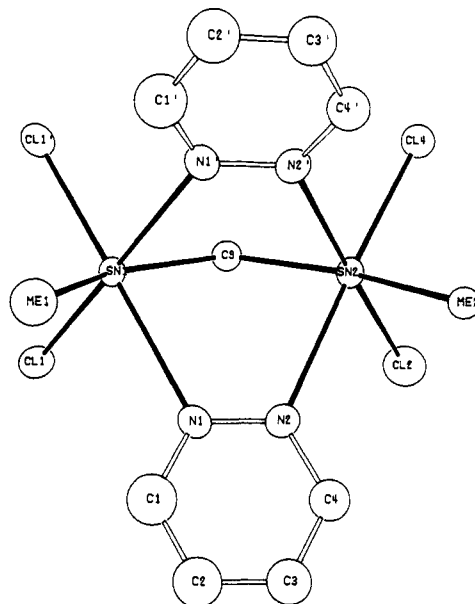


Figure 4. The structure of $[(\text{CH}_3)\text{Cl}_2\text{Sn}(\text{CH}_2)(\text{N}_2\text{C}_4\text{H}_4)_2\text{SnCl}_2-(\text{CH}_3)_3]$ (3).

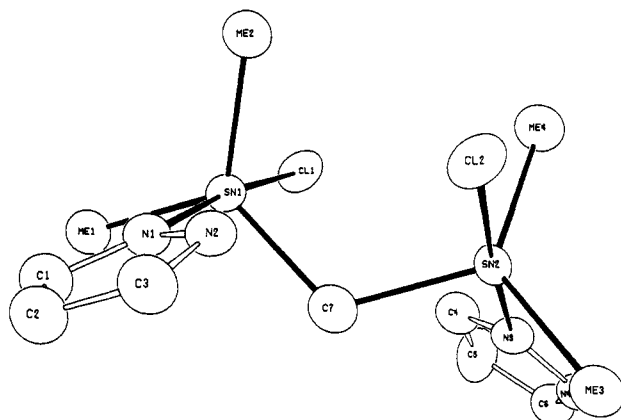


Figure 5. ORTEP view of the structure of $[(\text{CH}_3)_2\text{Cl}(\text{N}_2\text{C}_3\text{H}_3)\text{Sn}(\text{CH}_2)\text{Sn}(\text{N}_2\text{C}_3\text{H}_3)\text{Cl}(\text{CH}_3)_2]$ (4).

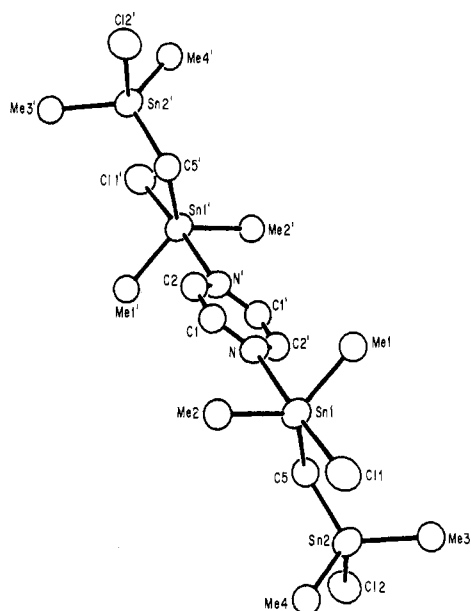


Figure 6. The structure of the tetranuclear species $[(\text{CH}_3)_2\text{ClSn}(\text{CH}_2)\text{SnCl}(\text{CH}_3)_2]_2(\text{N}_2\text{C}_4\text{H}_4)$ (5).

electronegative groups occupy axial positions of the trigonal bipyramid. Sn(2) also displays trigonal-bipyramidal

Table I. Comparison of Selected Bond Lengths (Å) for SnC₃XY Trigonal-Bipyramidal Sn Centers of 1, 2, 4, and 5

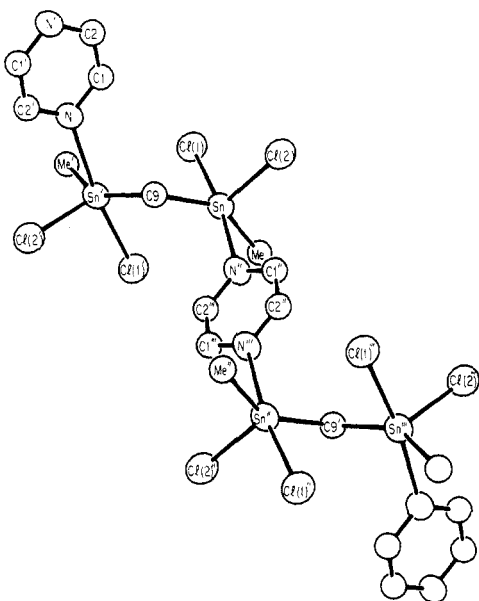
Sn center	Sn-C1	Sn-C2	Sn-C3(bridge) ^a	Sn-X ^b	Sn-Y ^b	location in Figure 8 ^c
Sn1 in 1	2.100 (10)	2.130 (17)	2.125 (1)	2.468 (2) (Cl)	3.009 (3) (Cl)	1
Sn2 in 1	2.148 (11)	2.089 (12)	2.099 (8)	2.638 (3) (Cl)	2.439 (9) (N)	2
Sn1 in 2	2.130 (8)	2.128 (8)	2.115 (7)	2.473 (2) (Cl)	2.651 (6) (N)	3
Sn2 in 2	2.129 (8)	2.125 (8)	2.129 (7)	2.456 (2) (Cl)	2.715 (6) (N)	4
Sn1 in 4	2.154 (16)	2.162 (20)	2.114 (14)	2.578 (4) (Cl)	2.459 (15) (N)	5
Sn2 in 4	2.106 (18)	2.132 (17)	2.142 (14)	2.603 (5) (Cl)	2.453 (14) (N)	6
Sn1 in 5	2.120 (15)	2.128 (18)	2.120 (15)	2.524 (6) (Cl)	2.622 (14) (N)	7
Sn2 in 5	2.113 (20)	2.085 (22)	2.112 (18)	2.437 (5) (Cl)	3.181 (4) (Cl)	8

^aC3 refers to the bridging methylene group. ^bX and Y occupy the axial positions of the trigonal bipyramid. Identity of X and Y given in parentheses. ^cRefers to Δd_x and Δd_y, as calculated from eq 1.

Table II. Comparison of Selected Bond Lengths (Å) for SnC₂X₂Y₂ Octahedral Centers of 3, 6, and 7

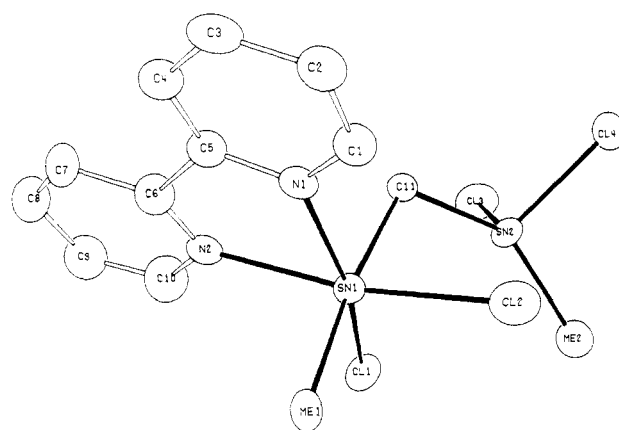
center	Sn-C1	Sn-C2-(bridge) ^a	Sn-X ^b	Sn-Y	Xn-X'	Sn-Y'	Sn-Y'	point in Figure 9 ^d
1 of 3	2.106 (13)	2.124 (10)	2.434 (1) (Cl)	2.608 (5) (N)	2.434 (1) (Cl)	2.608 (5) (N)	2.608 (5) (N)	1
2 of 3	2.121 (8)	2.111 (7)	2.457 (2) (Cl)	2.599 (6) (N)	2.457 (2) (Cl)	2.599 (6) (N)	2.599 (6) (N)	2
1 of 6	2.115 (11)	2.098 (6)	2.482 (2) (Cl)	2.540 (7) (N)	2.360 (3) (Cl)	3.269 (2) (Cl)	3.269 (2) (Cl)	3
1 of 7 ^c	2.047 (32)	2.160 (32)	2.609 (10) (Cl)	2.609 (10) (Cl)	2.577 (11) (Cl)	2.577 (11) (Cl)	2.372 (34) (N)	4
2 of 7	2.090 (32)	2.086 (33)	2.377 (10) (Cl)	3.290 (10) (Cl)	2.382 (10) (Cl)	3.382 (10) (Cl)	3.235 (10) (Cl)	5

^aC3 refers to the bridging methylene group. ^bX is trans to Y; X' is trans to Y'; identity of X, Y, X', and Y' in parentheses. ^cSn1 and Sn2 of 6 are identical by symmetry. ^dRefers to Δd_x and Δd_y, as calculated from eq 1.

**Figure 7.** A view of part of the one-dimensional zigzag chain of the polymeric structure of $[(\text{CH}_2(\text{Cl}_2\text{MeSn})_2\text{N}_2\text{C}_4\text{H}_4)_n]$ (6).

geometry, again with carbon atoms Me(3), Me(4), and C(6) in the equatorial plane and the axial positions occupied by Cl(2) and N(1) from the pyridazine group. The Sn(2)–Cl(2) bond distance of 2.638 (3) Å is considerably longer than the Sn(1)–Cl(1) distance of 2.468 (2) Å, an observation consistent with structural trends in SnC₃XY centers. As the Sn–Y distance along the axis decreases, the Sn–X distance tends to become longer as predicted by structure correlation arguments advanced by Britton and Dunitz, which will be discussed in more detail below.⁵

Figure 3 shows the structure of the pyridazine adduct $[(\text{CH}_3)_2\text{ClSn}(\text{CH}_2)(\text{N}_2\text{C}_4\text{H}_4)\text{SnCl}(\text{CH}_3)_2]$ (2), that consists of discrete binuclear units with Sn centers bridged by a methylene group, C(5), and the N donors of the pyridazine ligand. The coordination geometry at the Sn centers is nearly identical, with the Sn atoms displaying trigonal-bipyramidal geometry. The equatorial plane for Sn(1) is defined by Me(1), Me(2), and C(5) at an average distance

**Figure 8.** ORTEP view of the structure of $[(\text{CH}_3)\text{Cl}(\text{bpy})\text{Sn}(\text{CH}_2)\text{SnCl}_2(\text{CH}_3)]$ (7).

of 2.121 (12) Å and Cl(1) and N(1) of the pyridazine group in the axial positions. The pyridazine group functions as a bridging ligand, forming symmetric bridges to the Sn centers through N(1) and N(2).

The structural consequences of introducing a second pyridazine group are illustrated in Figure 4, which shows the structure of $[(\text{CH}_3)_2\text{Cl}_2\text{Sn}(\text{CH}_2)(\text{N}_2\text{C}_4\text{H}_4)_2\text{SnCl}_2(\text{CH}_3)]$ (3). The discrete binuclear tin compound presents pseudo-octahedral Sn centers bridged by the methylene group C(9) and two symmetrically bound pyridazine ligands. The binuclear unit possesses mirror symmetry with Sn(1), Sn(2), Me(1), Me(2), and C(9) occupying the plane. The coordination polyhedron about the Sn centers is defined by the carbon atoms Me and C(9), two mirror-related Cl atoms, and the N donors from the bridging pyridazine groups. The pyridazine N atoms are trans to the Cl donors, while the bridging C(9) is situated trans to the methyl substituent. Transoid cations and approximate C_{2v} local symmetry are not uncommon for SnC₂X₂Y₂ ensembles.

Figure 5 illustrates the structure of the pyrazole adduct $[(\text{CH}_3)_2\text{Cl}(\text{N}_2\text{C}_3\text{H}_3)\text{Sn}(\text{CH}_2)\text{Sn}(\text{N}_2\text{C}_3\text{H}_3)\text{Cl}(\text{CH}_3)_2]$ (4). The discrete binuclear compound exhibits five-coordinate Sn centers of pseudo-trigonal-bipyramidal geometry, sharing a bridging methylene group, C(7). The equatorial plane of each Sn atom is defined by two methyl substituents and the bridging methylene carbon atom, while the axial positions are occupied by a Cl atom and the N donor of

(5) Britton, D.; Dunitz, J. D. *J. Am. Chem. Soc.* 1981, 103, 2971.

Table III. Summary of Experimental Details and Crystal Data for the Structures Studied^a

	1	2	3	4	5	6	7
(A) Crystal Parameters at 23 °C ^a							
<i>a</i> , Å	7.192 (2)	9.330 (2)	8.758 (2)	10.178 (2)	6.939 (2)	9.964 (2)	12.845 (3)
<i>b</i> , Å	10.175 (2)	17.224 (3)	13.111 (3)	10.365 (2)	9.624 (2)	12.414 (3)	11.617 (2)
<i>c</i> , Å	12.853 (3)	9.860 (2)	16.366 (3)	17.670 (3)	10.460 (2)	12.510 (3)	15.361 (3)
α, deg	111.76 (1)	90.00	90.0	90.00	102.21 (1)	90.00	90.00
β, deg	95.09 (1)	97.78 (1)	90.0	90.0	92.38 (1)	90.00	95.45 (1)
γ, deg	105.40 (1)	90.00	90.00	90.00	90.39 (1)	90.00	90.00
<i>V</i> , Å ³	823.5 (8)	1569.9 (9)	1879.2 (9)	1864.0 (8)	680.4 (8)	1547.3 (9)	2281.8 (10)
space group	<i>P</i> $\bar{1}$	<i>P</i> 2 ₁ / <i>n</i>	<i>Pnam</i>	<i>P</i> 2 ₁ 2 ₁ 2 ₁	<i>P</i> $\bar{1}$	<i>Pbn</i> <i>b</i>	<i>P</i> 2 ₁ / <i>n</i>
<i>Z</i>	2	4	4	4	1	4	4
<i>D</i> (calcd), g cm ⁻³	1.86	1.96	2.06	1.84	2.03	2.04	1.69
(B) Measurement of Intensity Data							
crystal dimens, mm	0.25 × 0.20 × 0.25	0.31 × 0.29 × 0.25	0.20 × 0.19 × 0.18	0.21 × 0.19 × 0.16	0.30 × 0.25 × 0.25	0.19 × 0.16 × 0.16	0.15 × 0.14 × 0.19
instrument	Nicolet R3m						
radiatn	Mo Kα (λ = 0.71030 Å)						
scan mode	coupled θ (crystal)-/2θ (counter)						
scan rate, deg/min	7-30						
scan range, deg	0 1 2θ ≤ 45						
scan length, deg	from [2θ(Kα ₁) - 1.0] to [2θ(Kα ₂) + 1.0]						
octants collected	+ <i>h</i> , ± <i>k</i> , ± <i>l</i>	+ <i>h</i> , + <i>k</i> , ± <i>l</i>	+ <i>h</i> , + <i>k</i> , + <i>l</i>	+ <i>h</i> , + <i>k</i> , + <i>l</i>	+ <i>h</i> , ± <i>k</i> , ± <i>l</i>	+ <i>h</i> , + <i>k</i> , + <i>l</i>	+ <i>h</i> , + <i>k</i> , ± <i>l</i>
bkgd measmt	stationary crystal, stationary counter; t the beginning and end of each 2θ scan; each for the time taken for the scan						
stds	3 collected every 197						
no. of reflctns collected	2911	2280	1150	1401	1971	1200	3165
no. of independent reflctns used in soln (<i>I</i> ≥ 3σ(<i>I</i>))	1691	1865	815	1195	1518	860	1344
(C) Reduction of Intensity Data and Summary of Structure Solution and Refinement ^{b,h}							
abs coeff, cm ⁻¹ (Mo Kα)	35.51	35.11	32.56	44.64	44.86	39.20	53.22
abs corr	empirical, based on ψ scans for 5 reflections with χ near 90°						
<i>T</i> _{max} / <i>T</i> _{min}	1.06	1.11	1.04	1.09	1.14	1.09	1.11
structure soln	in all cases, Sn positions were determined from a Patterson map; all other atomic positions were located on subsequent difference Fourier maps						
atom scattering factors ^c	neutral atomic scattering factors were used throughout the analysis						
anomalous dispersion ^d	applied to all non-hydrogen atoms						
final discrepancy factor ^e							
<i>R</i>	0.037	0.036	0.026	0.046	0.026	0.022	0.051
<i>R</i> _w	0.039	0.039	0.025	0.046	0.027	0.028	0.049
goodness of fit ^f	1.94	1.62	1.25	2.01	1.81	1.17	1.18

^a From a least-squares fitting of the setting angle of 25 reflections. ^b All calculations were performed on a Data General Nova 3 computer with 32K of 16-bit words using local versions of the Nicolet SHELXTL interactive crystallographic software package as described in: Sheldrick, G. M. *Nicolet SHELXTL Operations Manual*; Nicolet XRD Corp.: Cupertino, CA, 1979. ^c Cromer, D. T.; Mann, J. B. *Acta Crystallogr., Sect. A: Cryst. Phys. Diffr.*, **1968**, *A24*, 321. ^d *International Tables for X-ray Crystallography*; Kynock Press: Birmingham, England, 1962; Vol. III. ^e *R* = Σ[|*F*_o| - |*F*_c|]; *R*_w = [Σ*w*(|*F*_o| - |*F*_c|)² / Σ*w*|*F*_o|²]^{1/2} with *w* = 1/σ²(*F*_o) + *g*(*F*_o); *g* = 0.001. ^f GOF = [Σ*w*(|*F*_o| - |*F*_c|)² / (NO - NV)]^{1/2} where NO is the number of observations and NV is the number of variables. ^g 1, [(CH₃)₂ClSn(CH₂)Sn(CH₂)₂(NC₅H₅)Cl]; 2, [(CH₃)₂ClSn(CH₂)(N₂C₄H₄)SnCl(CH₂)₂]; 3, [(CH₃)Cl₂Sn(CH₂)(N₂C₄H₄)SnCl₂(CH₃)]; 4, [(CH₃)₂ClSn(CH₂)(N₂C₃H₃)Sn(CH₂)₂(N₂C₄H₄)]; 5, [(CH₃)₂ClSn(CH₂)SnCl(CH₂)₂(N₂C₄H₄)]; 6, [CH₂(Cl₂MeSn)₂(N₂C₄H₄)]; 7, [(CH₃)Cl(bpy)Sn(CH₂)SnCl₂(CH₃)₂]. ^h Data corrected for background, attenuation, Lorentz, and polarization effects in the usual fashion.

Table IV. Bond Lengths (Å) for [(CH₃)₂ClSn(CH₂)Sn(NC₅H₅)(CH₂)₂Cl] (1)

Sn(1)-Cl(1)	2.468 (2)	Sn(1)-Cl(2)	3.009 (3)
Sn(1)-C(6)	2.125 (10)	Sn(1)-Me(1)	2.100 (10)
Sn(1)-Me(2)	2.130 (17)	Sn(2)-Cl(2)	2.638 (3)
Sn(2)-N(1)	2.439 (9)	Sn(2)-C(6)	2.099 (8)
Sn(2)-Me(3)	2.148 (11)	Sn(2)-Me(4)	2.089 (12)
C(1)-C(2)	1.385 (20)	C(1)-N(1)	1.328 (17)
C(2)-C(3)	1.406 (25)	C(3)-C(4)	1.367 (24)
C(4)-C(5)	1.349 (20)	C(5)-N(1)	1.345 (14)

the pyrazole ligand. This represents the anticipated geometry for SnC₃XY type center.

Adduct formation with the pyrazine group results in gross structural consequences, as illustrated in Figure 6, which displays the structure of [(CH₃)₂ClSn(CH₂)SnCl(CH₂)₂(N₂C₄H₄) (5)]. The structure consists of two binuclear, methylene-bridged [(CH₃)₂ClSn(CH₂)SnCl(CH₂)₂] units, in turn bridged through the nitrogen donors of the pyrazine group to give a tetranuclear Sn species. The inversion center at the centroid of the pyrazine ring relates the binuclear fragments of the tetranuclear unit. Two distinct trigonal-bipyramidal Sn environments are present:

Table V. Bond Angles (deg) for [(CH₃)₂ClSn(CH₂)Sn(NC₅H₅)(CH₂)₂Cl] (1)

Cl(1)-Sn(1)-Cl(2)	176.3 (1)	Cl(1)-Sn(1)-C(6)	97.7 (2)
Cl(2)-Sn(1)-C(6)	78.6 (2)	Cl(1)-Sn(1)-Me(1)	96.7 (3)
Cl(2)-Sn(1)-Me(1)	84.7 (3)	C(6)-Sn(1)-Me(1)	120.1 (4)
Cl(1)-Sn(1)-Me(2)	95.4 (3)	Cl(2)-Sn(1)-Me(2)	86.8 (3)
C(6)-Sn(1)-Me(2)	116.8 (5)	Me(1)-Sn(1)-Me(2)	119.2 (5)
Cl(2)-Sn(2)-N(1)	175.4 (2)	Cl(2)-Sn(2)-C(6)	88.4 (3)
N(1)-Sn(2)-C(6)	88.0 (3)	Cl(2)-Sn(2)-Me(3)	92.6 (3)
N(1)-Sn(2)-Me(3)	87.0 (4)	C(6)-Sn(2)-Me(3)	122.1 (4)
Cl(2)-Sn(2)-Me(4)	89.8 (3)	N(1)-Sn(2)-Me(4)	94.4 (4)
C(6)-Sn(2)-Me(4)	11.9 (4)	Me(3)-Sn(2)-Me(4)	118.0 (4)
Sn(1)-Cl(2)-Sn(2)	77.6 (1)	C(2)-C(1)-N(1)	123.6 (14)
C(1)-C(2)-C(3)	116.2 (16)	C(2)-C(3)-C(4)	120.2 (14)
C(3)-C(4)-C(5)	118.8 (14)	C(4)-C(5)-N(1)	123.3 (12)
Sn(2)-N(1)-C(1)	117.3 (7)	Sn(2)-N(1)-C(5)	124.9 (8)
C(1)-N(1)-C(5)	117.8 (10)	Sn(1)-C(6)-Sn(2)	114.4 (3)

Sn(2) presents three carbon atoms Me(3), Me(4), and C(5) in the equatorial plane with Cl(2) and Cl(1) in the apical positions at distances of 2.437 (5) and 3.181 (5) Å, respectively. The geometry is similar to that displayed by Sn(1) of 1. On the other hand, Sn(1) also possesses a trigonal plane of carbon atoms, Me(1), Me(2), and C(5),

Table VI. Bond Lengths (Å) for $[(CH_3)_2Cl_2Sn(CH_2)(N_2C_4H_4)SnCl(CH_3)_2]$ (2)

Sn(1)-Cl(1)	2.473 (2)	Sn(1)-N(1)	2.651 (6)
Sn(1)-C(5)	2.115 (7)	Sn(1)-Me(1)	2.130 (8)
S(1)-Me(2)	2.128 (8)	Sn(2)-Cl(2)	2.456 (2)
Sn(2)-N(2)	2.715 (6)	Sn(2)-C(5)	2.129 (7)
Sn(2)-Me(3)	2.129 (8)	Sn(2)-Me(4)	2.125 (8)
N(1)-N(2)	1.317 (8)	N(1)-C(1)	1.322 (10)
N(2)-C(4)	1.322 (10)	C(11)-C(2)	1.360 (13)
C(12)-C(3)	1.338 (15)	C(13)-C(4)	1.362 (13)

Table VII. Bond Angles (deg) for $[(CH_3)_2Cl_2Sn(CH_2)(N_2C_4H_4)SnCl(CH_3)_2]$ (2)

Cl(1)-Sn(1)-N(1)	177.6 (2)	Cl(1)-Sn(1)-C(5)	98.6 (2)
N(1)-Sn(1)-C(5)	82.6 (2)	Cl(1)-Sn(1)-Me(1)	96.8 (2)
N(1)-Sn(1)-Me(1)	80.8 (2)	C(1)-Sn(1)-Me(1)	120.4 (3)
Cl(1)-Sn(1)-Me(2)	95.3 (2)	N(1)-Sn(1)-Me(2)	86.0 (2)
C(5)-Sn(1)-Me(2)	115.3 (3)	Me(1)-Sn(1)-Me(2)	120.0 (3)
Cl(2)-Sn(2)-N(2)	177.7 (1)	Cl(2)-Sn(2)-C(5)	96.9 (2)
N(2)-Sn(2)-C(5)	80.9 (2)	Cl(2)-Sn(2)-Me(3)	96.5 (2)
N(2)-Sn(2)-Me(3)	84.9 (2)	C(5)-Sn(2)-Me(3)	119.1 (3)
Cl(2)-Sn(2)-Me(4)	97.3 (3)	N(2)-Sn(2)-Me(4)	83.5 (3)
C(5)-Sn(2)-Me(4)	118.8 (3)	Me(3)-Sn(2)-Me(4)	117.9 (3)
Sn(1)-N(1)-N(2)	114.8 (4)	Sn(1)-N(1)-C(1)	125.3 (5)
N(2)-N(1)-C(1)	119.1 (6)	Sn(2)-N(2)-N(1)	117.2 (4)
Sn(2)-N(2)-C(4)	125.2 (5)	N(1)-N(2)-C(4)	117.5 (6)
N(1)-C(1)-C(2)	124.9 (8)	C(1)-C(2)-C(3)	116.0 (8)
C(2)-C(3)-C(4)	117.9 (9)	N(2)-C(4)-C(3)	124.5 (8)
Sn(1)-C(5)-Sn(2)	120.2 (4)		

Table VIII. Bond Lengths (Å) for $[(CH_3)_2Cl_2Sn(CH_2)(N_2C_4H_4)_2SnCl_2(CH_3)]$ (3)

Sn(1)-Cl(1)	2.434 (1)	Sn(1)-N(1)	2.608 (5)
Sn(1)-C(9)	2.124 (10)	Sn(1)-Me(1)	2.106 (13)
Sn(2)-Cl(2)	2.457 (2)	Sn(2)-N(2)	2.599 (6)
Sn(2)-Me(2)	2.121 (8)	Sn(2)-C(9)	2.111 (7)
N(2)-N(1)	1.304 (8)	N(2)-C(4)	1.332 (8)
N(1)-C(1)	1.327 (10)	C(3)-C(2)	1.310 (12)
C(3)-C(4)	1.359 (11)	C(2)-C(1)	1.356 (9)

Table IX. Bond Angles (deg) for $[(CH_3)_2Cl_2Sn(CH_2)(N_2C_4H_4)_2SnCl_2(CH_3)]$ (3)

Cl(1)-S(1)-N(1)	84.2 (1)	Cl(1)-Sn(1)-C(9)	99.5 (1)
N(1)-Sn(1)-C(9)	80.8 (2)	Cl(1)-Sn(1)-Me(1)	98.1 (2)
N(1)-Sn(1)-Me(1)	81.8 (2)	C(9)-Sn(1)-Me(1)	153.7 (3)
Cl(1)-Sn(1)-Cl(1')	95.3 (1)	N(1)-Sn(1)-Cl(1')	179.5 (1)
C(9)-Sn(1)-Cl(1')	99.5 (1)	Me(1)-Sn(1)-Cl(1')	98.1 (2)
Cl(1)-Sn(1)-N(1')	179.5 (1)	N(1)-Sn(1)-N(1')	96.3 (2)
C(9)-Sn(1)-N(1')	80.8 (2)	Me(1)-Sn(1)-N(1')	81.8 (2)
Cl(1')-Sn(1)-N(1')	84.2 (1)	Cl(2)-Sn(2)-N(2)	84.1 (1)
Cl(2)-Sn(2)-Me(2)	95.2 (2)	N(2)-Sn(2)-Me(2)	83.8 (2)
Cl(2)-Sn(2)-C(9)	98.9 (2)	N(2)-Sn(2)-C(9)	81.8 (2)
Me(2)-Sn(2)-C(9)	158.6 (4)	Cl(2)-Sn(2)-Cl(2')	96.9 (1)
N(2)-Sn(2)-Cl(2')	178.6 (1)	Me(2)-Sn(2)-Cl(2')	95.2 (2)
C(9)-Sn(2)-Cl(2')	98.9 (2)	Cl(2)-Sn(2)-N(2')	178.6 (1)
N(2)-Sn(2)-N(2')	94.8 (3)	Me(2)-Sn(2)-N(2')	83.8 (2)
C(9)-Sn(2)-N(2')	81.8 (2)	Cl(2)-Sn(2)-N(2')	84.1 (1)
Sn(2)-N(2)-N(1)	116.8 (3)	Sn(2)-N(2)-C(4)	124.8 (5)
N(1)-N(2)-C(4)	118.4 (6)	Sn(1)-N(1)-N(2)	117.3 (4)
Sn(1)-N(1)-C(1)	123.3 (4)	N(2)-N(1)-C(1)	119.3 (5)
Sn(1)-C(9)-Sn(2)	120.5 (4)	C(2)-C(3)-C(4)	117.4 (6)
C(3)-C(2)-C(1)	118.6 (8)	N(2)-C(4)-C(3)	123.4 (7)
N(1)-C(1)-C(2)	122.7 (7)	Sn(2)-N(2)-N(1')	116.8 (3)
Sn(1)-N(1)-N(2')	117.3 (4)		

but displays Cl(1) and the pyrazine donor N(1) in the apical positions. The structure illustrates the general tendency of pyridazine and pyrazine to coordinate through both N donors. Thus, while pyridazine will symmetrically bridge Sn centers of a binuclear unit, the pyrazine ligand must bridge adjacent binuclear centers to form tetranuclear units or high oligomers.

The tendency of the pyrazine group to bridge through the nitrogen donors results in a polymeric 2:1 adduct, $CH_2(Cl_2MeSn)_2 \cdot N_2C_4H_4$ (6), whose structure is shown in Figure 7. The tin centers are related by a twofold axis

Table X. Bond Lengths (Å) for $[(CH_3)_2Cl(N_2C_3H_3)Sn(CH_2)Sn(N_2C_3H_3)Cl(CH_3)_2]$ (4)

Sn(1)-Cl(1)	2.578 (4)	Sn(1)-C(7)	2.114 (14)
Sn(1)-N(1)	2.459 (15)	Sn(1)-Me(2)	2.162 (20)
Sn(1)-Me(1)	2.154 (16)	Sn(2)-Cl(2)	2.603 (5)
Sn(2)-C(7)	2.142 (14)	Sn(2)-N(3)	2.453 (14)
Sn(2)-Me(3)	2.106 (18)	Sn(2)-Me(4)	2.132 (17)
Cl(1)-Sn(1)	2.578 (4)	C(7)-Sn(1)	2.114 (14)
N(3)-C(4)	1.280 (18)	N(3)-N(4)	1.338 (23)
N(1)-N(2)	1.352 (21)	N(1)-C(1)	1.319 (23)
N(1)-Sn(1)	2.459 (15)	C(4)-C(5)	1.307 (25)
N(4)-C(6)	1.377 (28)	C(2)-C(3)	1.302 (26)
C(2)-C(1)	1.398 (27)	N(2)-C(3)	1.327 (23)
C(6)-C(5)	1.368 (29)	Me(2)-Sn(1)	2.162 (20)
Me(1)-Sn(1)	2.154 (16)	Sn(1)-C(7)	2.114 (14)
Sn(1)-N(1)	2.459 (15)	Sn(1)-Me(2)	2.162 (20)
Sn(1)-Me(1)	2.154 (16)	C(7)-Sn(1)	2.114 (14)
N(1)-Sn(1)	2.459 (15)	Me(2)-Sn(1)	2.162 (20)
Me(1)-Sn(1)	2.154 (16)		

Table XI. Bond Angles (deg) for $[(CH_3)_2Cl(N_2C_3H_3)Sn(CH_2)Sn(N_2C_3H_3)Cl(CH_3)_2]$ (4)

Cl(1)-Sn(1)-C(7)	90.5 (4)	Cl(1)-Sn(1)-N(1)	174.6 (4)
C(7)-Sn(1)-N(1)	84.2 (5)	Cl(1)-Sn(1)-Me(2)	94.0 (5)
C(7)-Sn(1)-Me(2)	119.9 (7)	N(1)-Sn(1)-Me(2)	87.7 (6)
Cl(1)-Sn(1)-Me(1)	94.1 (5)	C(7)-Sn(1)-Me(1)	121.9 (6)
N(1)-Sn(1)-Me(1)	89.7 (6)	Me(2)-Sn(1)-Me(1)	117.6 (7)
Cl(2)-Sn(2)-C(7)	92.7 (4)	Cl(2)-Sn(2)-N(3)	176.1 (3)
C(7)-Sn(2)-N(3)	90.5 (5)	Cl(2)-Sn(2)-Me(3)	92.2 (5)
C(7)-Sn(2)-Me(3)	111.6 (6)	N(3)-Sn(2)-Me(3)	88.7 (6)
Cl(2)-Sn(2)-Me(4)	90.0 (5)	C(7)-Sn(2)-Me(4)	121.4 (6)
N(3)-Sn(2)-Me(4)	86.5 (5)	Me(3)-Sn(2)-Me(4)	126.7 (7)
Sn(2)-C(7)-Sn(1)	118.0 (6)	Sn(2)-N(3)-C(4)	122.1 (10)
Sn(2)-N(3)-N(4)	131.8 (12)	C(4)-N(3)-N(4)	106.1 (14)
N(2)-N(1)-C(1)	106.1 (15)	N(2)-N(1)-Sn(1)	120.9 (11)
C(1)-N(1)-Sn(1)	132.4 (12)	N(3)-C(4)-C(5)	112.7 (14)
N(3)-N(4)-C(6)	109.5 (17)	C(3)-C(2)-C(1)	107.2 (16)
N(1)-N(2)-C(3)	110.1 (15)	C(2)-C(3)-N(2)	108.3 (16)
N(1)-C(1)-C(2)	108.3 (16)	N(4)-C(6)-C(5)	103.9 (19)
C(4)-C(5)-C(6)	107.4 (16)	Cl(1)-Sn(1)-C(7)	90.5 (4)
Cl(1)-Sn(1)-N(1)	174.6 (4)	C(7)-Sn(1)-N(1)	84.2 (5)
Cl(1)-Sn(1)-Me(2)	94.0 (5)	C(7)-Sn(1)-Me(2)	119.9 (7)
N(1)-Sn(1)-Me(2)	87.7 (6)	Cl(1)-Sn(1)-Me(1)	94.1 (5)
C(7)-Sn(1)-Me(1)	121.9 (6)	N(1)-Sn(1)-Me(1)	89.7 (6)
Me(2)-Sn(1)-Me(1)	117.6 (7)		

Table XII. Bond Lengths (Å) for $[(CH_3)_2Cl_2Sn(CH_2)SnCl(CH_3)_2(N_2C_4H_4)]$ (5)

Sn(1)-Cl(1)	2.524 (6)	Sn(1)-N(1)	2.622 (14)
Sn(1)-C(5)	2.120 (15)	Sn(1)-Me(2)	2.128 (18)
Sn(1)-Me(1)	2.184 (20)	Sn(2)-Cl(2)	2.437 (5)
Sn(2)-C(5)	2.112 (8)	Sn(2)-Me(3)	2.113 (20)
Sn(2)-Me(4)	2.085 (22)	N(1)-C(1)	1.326 (22)
N(1)-C(2)	1.327 (21)	C(1)-C(2)	1.310 (28)
C(2)-N(1)	1.327 (21)	Sn(2)-Cl(1)	3.181 (4)

Table XIII. Bond Angles (deg) for $[(CH_3)_2Cl_2Sn(CH_2)SnCl(CH_3)_2(N_2C_4H_4)]$ (5)

Cl(1)-Sn(1)-N(1)	176.2 (3)	Cl(1)-Sn(1)-C(5)	93.3 (5)
N(1)-Sn(1)-C(5)	89.0 (6)	Cl(1)-Sn(1)-Me(2)	95.6 (6)
N(1)-Sn(1)-Me(2)	86.3 (6)	C(5)-Sn(1)-Me(2)	113.7 (7)
Cl(1)-Sn(1)-Me(1)	97.2 (6)	N(1)-Sn(1)-Me(1)	79.0 (7)
C(5)-Sn(1)-Me(1)	118.4 (7)	Me(2)-Sn(1)-Me(1)	125.3 (7)
Cl(2)-Sn(2)-C(5)	99.6 (4)	Cl(2)-Sn(2)-Me(3)	99.6 (5)
C(5)-Sn(2)-Me(3)	119.8 (8)	Cl(2)-Sn(2)-Me(4)	98.7 (5)
C(5)-Sn(2)-Me(4)	117.4 (8)	Me(3)-Sn(2)-Me(4)	115.1 (9)
Sn(1)-N(1)-C(1)	124.5 (11)	Sn(1)-M(1)-C(2)	119.8 (11)
C(1)-N(1)-C(2)	115.7 (16)	N(1)-C(1)-C(2)	122.9 (16)
Sn(1)-C(5)-Sn(2)	114.0 (8)	C(1)-C(2)-N(1)	121.4 (16)

Table XIV. Bond Lengths (Å) for $[CH_2(Cl_2MeSn)_2 \cdot N_2C_4H_4]_n$ (6)

Sn-Cl(1)	2.482 (2)	Sn-Cl(2)	2.360 (3)
Sn-N''	2.540 (7)	Sn-Me	2.115 (11)
Sn-C(9)	2.098 (6)	N-C(1)	1.332 (12)
N-C(1)	1.329 (12)	C(1)-C(2)	1.317 (13)
Sn-Cl(1)	3.269 (2)		

Table XV. Bond Angles (deg) for $[(CH_2)(Cl_2MeSn)_2 \cdot N_2C_4H_4]_n$ (6)

Cl(1)-Sn-Cl(2)	95.5 (1)	Cl(1)-Sn-N''	171.2 (2)
Cl(2)-Sn-N''	89.6 (2)	Cl(1)-Sn-Me	98.9 (3)
Cl(2)-Sn-Me	105.2 (3)	N''-Sn-Me	86.6 (3)
Cl(1)-Sn-C(9)	88.6 (2)	Cl(2)-Sn-C(9)	106.8 (2)
N-Sn-C(9)	83.1 (2)	Me-Sn-C(9)	146.2 (3)
Sn-N''-C(1')	118.4 (6)	Sn-N''-C(2')	126.7 (6)
C(1)-N-C(2')	114.8 (7)	N-C(1)-C(2)	123.9 (9)
C(1)-C(2)-N'	121.2 (8)	Sn-C(9)-Sn	109.6 (5)

Table XVI. Bond Lengths (Å) for $[(CH_3)Cl_2(bpy)Sn(CH_2)SnCl_2(CH_3)]$ (7)

Sn(2)-Cl(3)	2.377 (10)	Sn(2)-Cl(4)	2.382 (10)
Sn(2)-C(11)	2.086 (33)	Sn(2)-Me(2)	2.090 (32)
Sn(1)-Cl(1)	2.609 (10)	Sn(1)-Cl(2)	2.577 (11)
Sn(1)-N(1)	2.270 (26)	Sn(1)-Me(1)	2.047 (32)
Sn(1)-N(2)	2.372 (34)	Sn(1)-C(11)	2.160 (32)
N(1)-C(5)	1.443 (44)	N(1)-C(1)	1.354 (45)
C(5)-C(4)	1.285 (47)	C(5)-C(6)	1.578 (43)
C(8)-C(9)	1.749 (74)	C(8)-C(7)	1.492 (53)
C(1)-C(2)	1.529 (58)	C(9)-N(2)	1.593 (67)
C(7)-C(6)	1.360 (53)	N(2)-C(6)	1.339 (46)
C(3)-C(4)	1.316 (58)	C(3)-C(2)	1.385 (66)
S(2)-Cl(1)	3.290 (10)	Sn(2)-Cl(2)	3.235 (10)

Table XVII. Bond Angles (deg) for $[(CH_3)Cl_2(bpy)Sn(CH_2)SnCl_2(CH_3)]$ (7)

Cl(3)-Sn(2)-Cl(4)	97.0 (4)	Cl(3)-Sn(2)-C(11)	102.8 (10)
Cl(4)-Sn(2)-C(11)	105.1 (9)	Cl(3)-Sn(2)-Me(2)	101.1 (11)
Cl(4)-Sn(2)-Me(2)	103.1 (10)	C(11)-Sn(2)-Me(2)	140.1 (13)
Cl(1)-Sn(1)-Cl(2)	100.2 (3)	Cl(1)-Sn(1)-N(1)	162.5 (7)
Cl(2)-Sn(1)-N(1)	96.5 (7)	Cl(1)-Sn(1)-Me(1)	91.8 (9)
Cl(2)-Sn(1)-Me(1)	89.3 (10)	N(1)-Sn(1)-Me(1)	93.5 (11)
Cl(1)-Sn(1)-N(2)	91.6 (9)	Cl(2)-Sn(1)-N(2)	167.8 (9)
N(1)-Sn(1)-N(2)	71.5 (11)	Me(1)-Sn(1)-N(2)	93.4 (12)
Cl(1)-Sn(1)-C(11)	83.6 (9)	Cl(2)-Sn(1)-C(11)	84.0 (9)
N(1)-Sn(1)-C(11)	93.0 (11)	Me(1)-Sn(1)-C(11)	171.1 (13)
N(2)-Sn(1)-C(11)	94.3 (12)	Sn(1)-N(1)-C(5)	124.7 (18)
Sn(1)-N(1)-C(1)	120.8 (24)	C(5)-N(1)-C(1)	114.5 (28)
N(1)-C(5)-C(4)	128.2 (30)	N(1)-C(5)-C(6)	105.5 (25)
C(4)-C(5)-C(6)	126.3 (32)	C(9)-C(8)-C(7)	101.3 (34)
N(1)-C(1)-C(2)	114.8 (35)	C(8)-C(9)-N(2)	102.0 (30)
C(8)-C(7)-C(6)	109.0 (33)	Sn(1)-N(2)-C(9)	141.0 (26)
Sn(1)-N(2)-C(6)	114.8 (28)	C(9)-N(2)-C(6)	104.1 (32)
C(4)-C(3)-C(2)	114.5 (39)	C(5)-C(4)-C(3)	122.8 (38)
C(5)-C(6)-C(7)	113.2 (29)	C(5)-C(6)-N(2)	123.4 (32)
C(7)-C(6)-N(2)	123.4 (33)	Sn(2)-C(11)-Sn(1)	109.1 (14)
C(1)-C(2)-C(3)	124.9 (34)		

Table XVIII. Atom Coordinates ($\times 10^4$) and Temperature Factors ($\text{Å}^2 \times 10^3$) for $[(CH_3)_2ClSn(CH_2)Sn(NC_3H_5XCH_3)_2Cl]$ (1)

atom	x	y	z	U_{iso}
Sn(1)	3943 (1)	2341 (1)	5495 (1)	53 (1)
Sn(2)	3017 (1)	2186 (1)	8122 (1)	51 (1)
Cl(1)	3216 (4)	301 (3)	3569 (2)	72 (1)
Cl(2)	4725 (4)	4676 (3)	7900 (3)	87 (1)
C(1)	2562 (19)	-1178 (12)	7944 (10)	82 (6)
C(2)	1902 (27)	-2590 (14)	7938 (11)	109 (8)
C(3)	35 (25)	-3000 (14)	8200 (10)	97 (7)
C(4)	-1000 (22)	-2013 (15)	8472 (11)	101 (7)
C(5)	-210 (16)	-656 (12)	8466 (9)	75 (5)
N(1)	1554 (12)	-220 (9)	8204 (6)	59 (4)
C(6)	2487 (13)	1045 (9)	6334 (7)	53 (4)
Me(1)	7029 (14)	2996 (11)	5719 (9)	69 (5)
Me(2)	2396 (19)	3597 (14)	4989 (12)	98 (8)
Me(3)	5622 (15)	2417 (12)	9223 (9)	81 (5)
Me(4)	956 (15)	3115 (11)	8884 (8)	68 (5)

passing through the bridging methylene group C(9). In addition, the center of symmetry located at the centroid of the pyrazine ring relates binuclear units and generates a one-dimensional zigzag chain structure. The Sn coordination geometry is essentially pseudooctahedral. Five coordination sites are occupied by groups at unremarkable

Table XIX. Atom Coordinates ($\times 10^4$) and Temperature Factors ($\text{Å}^2 \times 10^3$) for $[(CH_3)_2ClSn(CH_2)(N_2C_4H_4)SnCl(CH_3)_2]$ (2)

atom	x	y	z	U_{iso}
Sn(1)	6596 (1)	1047 (1)	1932 (1)	42 (1)
Sn(2)	10135 (1)	2016 (1)	2156 (1)	45 (1)
Cl(1)	4507 (2)	1855 (1)	984 (3)	69 (1)
Cl(2)	10052 (2)	3400 (1)	1549 (3)	81 (1)
N(1)	8840 (6)	158 (3)	2846 (7)	53 (2)
N(2)	10112 (6)	489 (4)	2835 (7)	57 (2)
C(1)	8780 (10)	-593 (5)	3103 (9)	71 (3)
C(2)	9948 (12)	-1069 (5)	3360 (10)	78 (4)
C(3)	11239 (11)	-732 (5)	3357 (10)	80 (4)
C(4)	11271 (9)	45 (5)	3103 (10)	79 (4)
C(5)	8016 (7)	1946 (4)	2720 (8)	52 (2)
Me(1)	6888 (8)	480 (5)	70 (8)	64 (3)
Me(2)	5497 (8)	470 (4)	3397 (8)	62 (3)
Me(3)	11941 (8)	2091 (5)	3720 (9)	63 (3)
Me(4)	10497 (8)	1580 (5)	215 (8)	67 (3)

Table XX. Atom Coordinates ($\times 10^4$) and Temperature Factors ($\text{Å}^2 \times 10^3$) for $[(CH_3)_2Cl_2Sn(CH_2)(N_2C_4H_4)_2SnCl_2(CH_3)]$ (3)

atom	x	y	z	U_{iso}
Sn(1)	6223 (1)	-1105 (1)	7500	33 (1)
Sn(2)	3236 (1)	866 (1)	7500	33 (1)
Cl(1)	6195 (2)	-2356 (1)	6401 (1)	51 (1)
Cl(2)	1376 (2)	824 (1)	6376 (1)	49 (1)
N(1)	6263 (7)	222 (3)	6313 (3)	49 (2)
N(2)	5242 (7)	945 (3)	6331 (3)	42 (2)
C(1)	7292 (11)	211 (5)	5718 (4)	73 (3)
C(2)	7331 (12)	927 (5)	5121 (4)	63 (3)
C(3)	6345 (10)	1678 (5)	5147 (4)	60 (3)
C(4)	5290 (10)	1662 (5)	5755 (4)	62 (3)
C(9)	3880 (11)	-685 (5)	7500	33 (3)
Me(1)	8582 (15)	-793 (7)	7500	63 (4)
Me(2)	3484 (12)	2476 (6)	7500	47 (3)

Table XXI. Atom Coordinates ($\times 10^4$) and Temperature Factors ($\text{Å}^2 \times 10^3$) for $[(CH_3)_2Cl(N_2C_3H_3)Sn(CH_2)Sn(N_2C_3H_3)Cl(CH_3)_2]$ (4)

atom	x	y	z	U_{iso}
Sn(1)	380 (1)	-1181 (1)	1054 (1)	46 (1)
Sn(2)	7826 (1)	567 (1)	6903 (1)	43 (1)
Cl(1)	6060 (5)	1016 (5)	4857 (2)	64 (2)
Cl(2)	6952 (5)	2232 (5)	7884 (3)	72 (2)
N(1)	3362 (14)	1163 (14)	7242 (8)	62 (5)
N(2)	3941 (16)	1466 (14)	7907 (8)	74 (6)
N(3)	8762 (13)	-896 (12)	5956 (8)	56 (5)
N(4)	9779 (17)	-1719 (20)	5988 (11)	100 (8)
C(1)	2179 (17)	734 (22)	7413 (11)	74 (8)
C(2)	2046 (18)	750 (19)	8200 (11)	70 (7)
C(3)	3142 (18)	1193 (19)	8478 (10)	62 (7)
C(4)	8350 (13)	-931 (15)	5274 (7)	34 (5)
C(5)	8930 (19)	-1820 (23)	4869 (10)	82 (8)
C(6)	9898 (21)	2351 (23)	5306 (10)	89 (9)
C(7)	5888 (14)	97 (13)	6633 (8)	40 (5)
Me(1)	4821 (18)	3244 (15)	6144 (10)	65 (6)
Me(2)	2883 (19)	443 (21)	5498 (10)	80 (8)
Me(3)	8699 (18)	-565 (21)	7755 (9)	77 (7)
Me(4)	8733 (17)	2091 (16)	6283 (9)	63 (7)

distances, Cl(1), Cl(2), Me(1), C(9), and N'' of the pyrazine ligand. The sixth position is occupied by Cl(1') in an unsymmetrical bridge at a distance of 3.269 (3) Å from Sn(1). The tin center may be considered an example of $SnC_2X_2Y_2$ coordination of the type discussed above for 3.

As a bidentate chelating ligand, bipyridine is expected to bond to a single Sn center, as shown in Figure 8 for $[(CH_3)_2Cl_2(bipy)Sn(CH_2)SnCl_2(CH_3)]$ (7). The compound consists of discrete binuclear Sn units bridged by a methylene carbon C(11). The coordination geometry about Sn(1) is essentially octahedral with the bridging methylene C(11) trans to the methyl group Me(1) and the nitrogen donors of the bipyridine ligand trans to Cl(1) and Cl(2).

Table XXII. Atom Coordinates ($\times 10^4$) and Temperature Factors ($\text{\AA}^2 \times 10^3$) for $[(\text{CH}_3)_2\text{ClSn}(\text{CH}_2)\text{SnCl}(\text{CH}_3)_2]_2(\text{N}_2\text{C}_4\text{H}_4)$ (5)

atom	x	y	z	U_{iso}
Sn(1)	6841 (2)	-3249 (1)	7138 (1)	36 (1)
Sn(2)	8427 (2)	355 (1)	7743 (1)	37 (1)
Cl(1)	8224 (8)	-2268 (5)	5311 (5)	63 (2)
Cl(2)	8397 (8)	2286 (5)	9671 (5)	61 (2)
N(1)	5574 (19)	-4399 (14)	9009 (13)	36 (5)
C(1)	4117 (26)	-5326 (18)	8862 (18)	44 (6)
C(2)	3565 (25)	-5919 (17)	9806 (17)	43 (6)
C(5)	7126 (26)	-1275 (17)	8497 (16)	42 (6)
Me(1)	9020 (28)	-4859 (20)	7217 (22)	60 (8)
Me(2)	4025 (26)	-3651 (21)	6242 (19)	54 (7)
Me(3)	11416 (28)	303 (23)	7425 (20)	64 (8)
Me(4)	6755 (31)	1282 (21)	6456 (20)	60 (8)

Table XXIII. Atom Coordinates ($\times 10^4$) and Temperature Factors ($\text{\AA}^2 \times 10^3$) for $[\text{CH}_2(\text{Cl}_2\text{MeSn})_2 \cdot \text{N}_2\text{C}_4\text{H}_4]_n$ (6)

atom	x	y	z	U_{iso}
Sn	784	1913 (1)	2404 (1)	37 (1)
Cl(1)	1713 (3)	3031 (2)	3873 (2)	55 (1)
Cl(2)	-887 (3)	1078 (3)	3453 (2)	64 (1)
N(1)	197 (8)	669 (5)	862 (6)	40 (3)
C(1)	1012 (9)	643 (7)	18 (7)	43 (3)
C(2)	845 (9)	-3 (7)	-807 (7)	41 (3)
Me(1)	-229 (12)	3135 (8)	1543 (8)	71 (4)
C(9)	2500	939 (8)	2500	35 (4)

Table XXIV. Atom Coordinates ($\times 10^4$) and Temperature Factors ($\text{\AA}^2 \times 10^3$) for $[(\text{CH}_3)_2\text{Cl}(\text{bpy})\text{Sn}(\text{CH}_2)\text{SnCl}_2(\text{CH}_3)]$ (7)

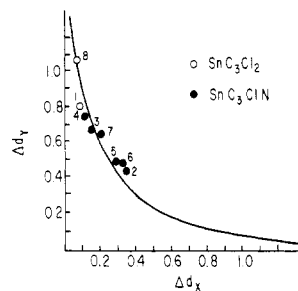
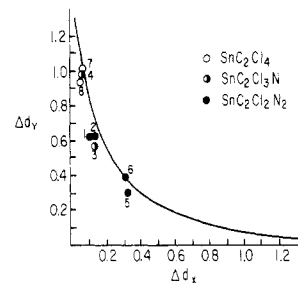
atom	x	y	z	U_{iso}
Sn(1)	-822 (2)	3789 (2)	2196 (1)	38 (1)
Sn(2)	-191 (2)	6474 (2)	1425 (1)	46 (1)
Cl(1)	752 (7)	4832 (9)	3060 (6)	70 (4)
Cl(2)	-2226 (8)	5374 (9)	2194 (6)	70 (4)
Cl(3)	1489 (7)	6961 (10)	1007 (6)	75 (4)
Cl(4)	-1189 (9)	7459 (9)	269 (6)	75 (4)
N(1)	-1793 (18)	2535 (25)	1325 (15)	49 (10)
N(2)	220 (35)	2153 (24)	1962 (18)	79 (16)
C(1)	-2775 (31)	2809 (38)	990 (20)	65 (17)
C(2)	-3329 (27)	1881 (44)	413 (20)	90 (20)
C(3)	-2922 (39)	803 (38)	263 (27)	102 (22)
C(4)	-1955 (26)	646 (34)	606 (22)	56 (15)
C(5)	-1443 (25)	1413 (29)	1074 (18)	49 (13)
C(6)	-273 (25)	1316 (32)	1486 (21)	49 (14)
C(7)	197 (29)	317 (34)	1276 (21)	55 (15)
C(8)	1307 (31)	331 (43)	1663 (26)	118 (22)
C(9)	1360 (41)	1645 (54)	2221 (20)	184 (30)
C(10)	1135 (13)	2025 (18)	2251 (12)	69 (8)
C(11)	-323 (26)	4733 (29)	1098 (20)	56 (14)
Me(1)	-1323 (29)	3139 (27)	3322 (19)	59 (14)
Me(2)	-291 (31)	7565 (30)	2496 (19)	73 (16)

The Sn(2) center also displays octahedral coordination, albeit rather more distorted. Four coordination sites display unremarkable distances, occupied by the bridging methylene group Cl(1), methyl carbon Me(2), Cl(3), and Cl(4). In addition, Sn(2) enjoys long contacts to the unsymmetrically bridging chloride atoms Cl(1) and Cl(2), 3.290 (3) and 3.235 (3) \AA, respectively. Both tin atoms display coordination geometries of the $\text{SnC}_2\text{X}_2\text{Y}_2$ -type with transoid carbon atoms.

Discussion

Structures 1-7 display two gross coordination sites for Sn, trigonal-bipyramidal and octahedral. Table I presents metrical parameters for the trigonal-bipyramidal Sn centers, and Table II presents those for the pseudo-octahedral sites.

As illustrated by the data in Table I, the trigonal-bipyramidal Sn centers display common structural features. All are of the SnC_3XY -type with approximate C_{3v} sym-

**Figure 9.** Δd_y vs. Δd_x for SnC_3XY ensembles.**Figure 10.** Δd_y vs. Δd_x for $\text{SnC}_2\text{X}_2\text{Y}_2$ ensembles.

metry. Hence, the equatorial plane in all cases is occupied by the carbon donor groups. Sn-C bond distances are remarkably similar whether the carbon is a terminal methyl carbon or a bridging methylene carbon. The usual covalent radii give a Sn-C distance of 2.10 \AA, in comparison to a value of 2.12 \AA for the average of 24 determinations in Table II. There is also a correlation along the X-Sn-Y axis: as the Sn-Y distance becomes shorter, the Sn-X distance tends to become longer. This correlation has been discussed in terms of the mapping of the $\text{S}_{\text{N}2}$ pathway with inversion of configuration between four- and five-coordinate Sn^{IV} . In general, there is a simple relationship between bond order and bond length

$$\Delta d(n) = d(n) - d(l) \quad (1)$$

where $d(n)$ is the bond length and $d(l)$ is the single bond length. Dunitz has plotted Δd_x and Δd_y for a number of SnC_3XY ensembles. Figure 9 shows the Dunitz curve⁶ with points marked indicating where our results fall on the theoretical line. The Sn centers display the common structural features. The large steric demands of the Cl groups are evident in the large Δd_y values for the SnC_3Cl_2 ensembles, points 1 and 8 on Figure 9.

A similar plot is presented in Figure 10 for the structural correlation of the $\text{SnC}_2\text{X}_2\text{Y}_2$ centers with transoid carbon groups, displaying local C_{2v} site symmetry. The relationship between Δd_x and Δd_y is similar to that for five-coordinate Sn. The Sn centers in structures 3, 6, and 7 display metrical parameters that are consistent with the structural trends summarized by the curve. These data have been interpreted in terms of the symmetric addition of two ligands Y to a tetrahedral SnC_2X_2 molecule, corresponding to an $\text{S}_{\text{N}3}$ reaction. The $\text{S}_{\text{N}3}$ path is not expected to be important in solution or the gas phase, as it requires a three-body collision. However, this path does define a valley in the potential energy surface and as such correlates the solid-state results.

The changes in the types of complexes formed with the nature of the reactants merits comment. For example, pyridine forms a 1:1 complex, 1, with bis(chlorodimethylstannyl)methane. A second pyridine could not be

(6) The curve is the bond order conservation function $10^{\Delta d_x/c} + 10^{-\Delta d_y/c} = 1$.

introduced with excess pyridine, as noted above. On the other hand, two pyrazole units coordinate with this chlorotin in **4** and halide bridging is absent ($\text{Sn}(1)\text{-Cl}(2) = 4.06 \text{ \AA}$) in the complex. The cause of this difference cannot be the relative basicities for pyrazole ($K_b = 3 \times 10^{-12}$) is a weaker base than pyridine ($K_b = 2.4 \times 10^{-9}$). Basicity should parallel donor ability because the σ orbitals of aromatic nitrogens are involved in each case. Another possible cause may be steric effects. In the five-membered ring of pyrazole the atoms bonded to the donor nitrogen are pinned back to internal angles of ca. 108° vs. 120° for pyridine. This is borne out in the angles between the acceptor tins, the donor nitrogen, and the neighboring atoms: in pyrazole the angles are $\text{Sn}(1)\text{-N}(1)\text{-C}(1) = 132^\circ$ and $\text{Sn}(1)\text{-N}(1)\text{-N}(2) = 120^\circ$, and in pyridine $\text{Sn}(2)\text{-N}(1)\text{-C}(1) = 117^\circ$ and $\text{Sn}(2)\text{-N}(1)\text{-C}(5) = 125^\circ$. These differences appear rather small to cause such a marked difference in the composition of the complexes. Structural factors in the crystal appear not to be the cause, however, because the 1:1 composition for pyridine is the only one observed in solution.

Pyrazine behaves like pyridine in that only one ligand coordinates to one bis(chlorodimethylstannyl)methane, but both nitrogens participate to form the 2:1 complex **5**. However, when the acceptor is the stronger acid, bis(dichloromethylstannyl)methane, both tin atoms act as acceptors and the polymeric structure **6** results. Pyridazine also shows a difference in behavior with the monochlorostannane (1:1 complex **2**) as compared to the dichloro analogue (2:1 complex). The axes of the σ orbitals on the nitrogens diverge at an angle of 60° ; this factor, coupled with appropriate bond lengths, leads to the novel mono- and bicyclic complexes that suffer minimal angle strain. Steric factors are undoubtedly the cause of the fact that bipyridyl chelates at only tin in **7**. If both tins were involved, the methylene group bridging the tins would form the apex shared by two very bulky octahedra.

Experimental Section

General Data. Proton nuclear resonance spectra were obtained at 60 MHz using a Varian EM-360A spectrometer. Chemical shifts are reported in parts per million downfield from internal tetramethylsilane followed in parentheses by the multiplicity, number of protons, coupling constant, and assignment. Proton-tin-119 coupling constants are reported as ${}^nJ(^{119}\text{Sn-H})$ with the first superscript denoting the number of bonds intervening between nuclei. Gas chromatographic analyses were performed on a Hewlett-Packard Model F & M 720 instrument using a 17 ft \times 0.25 in. copper column packed with 15% SE-30 on a Chromosorb W, 60-80 mesh. Melting points are uncorrected. Carbon-hydrogen analyses were done by Instranal of Rensselaer, NY, and Galbraith of Knoxville, TN.

Bis(chlorodimethylstannyl)methane (**1**) and bis(dichloromethylstannyl)methane (**2**) were prepared as previously described.²

Complexation of Bis(chlorodimethylstannyl)methane with Pyridine in Solution. Increments of pyridine were added to an 0.55 M solution of bis(chlorodimethylstannyl)methane in methylene chloride and the coupling constants for the methyl and methylene protons determined. The results are plotted in Figure 1.

Preparation of Complexes with Bis(chlorodimethylstannyl)methane. With Pyridine. To a solution of 1.50 g (3.93 mmol) of the stannylmethane was added 0.311 g (3.93 mmol) of pyridine. The resulting solution was concentrated to about 5 mL and placed in a refrigerator overnight whereupon crystals of **1** appeared: 1.37 g (75%); mp 98-99 $^\circ\text{C}$; ${}^1\text{H NMR}$ (CH_2Cl_2) δ 0.83 (${}^2J(^{119}\text{Sn-CH}_3) = 65 \text{ Hz}$), 1.22 ($J(^{119}\text{Sn-CH}_2) = 67 \text{ Hz}$).

Anal. Calcd for $\text{C}_{10}\text{H}_{19}\text{Cl}_2\text{NSn}_2$: C, 26.03; H, 4.15. Found: C, 25.96; H, 4.46.

With Pyridazine. A solution containing 2.0 g (5.2 mmol) of the stannylmethane and 0.39 g (5.87 mmol) of pyridazine in 10 mL of benzene was heated and concentrated until crystallization

began. Crystals of **2** appeared upon cooling: mp 111-112 $^\circ\text{C}$; ${}^1\text{H NMR}$ δ 0.77 (${}^2J(^{119}\text{Sn-CH}_3) = 66 \text{ Hz}$), 1.1 (${}^2J(^{119}\text{Sn-C}_2) = 69 \text{ Hz}$). Anal. Calcd for $\text{C}_9\text{H}_{12}\text{Cl}_2\text{N}_2\text{Sn}_2$: C, 23.37; H, 3.92. Found: C, 23.29; H, 3.96.

With Bipyridyl. A minimum volume of boiling benzene was used to dissolve 2.00 g (5.23 mmol) of the stannylmethane and 1.80 g (10.3 mmol) of bipyridyl. To this solution was added CCl_4 until it became cloudy. Cooling in the refrigerator overnight resulted in the appearance of 0.45 g of a product that was crystallized from CH_2Cl_2 : mp 136-137 $^\circ\text{C}$; ${}^1\text{H NMR}$ (CH_2Cl_2) δ 0.35 (${}^2J(^{119}\text{Sn-CH}_3) = 68 \text{ Hz}$), 0.55 (${}^2J(^{119}\text{Sn-CH}_3) = 114 \text{ Hz}$), 1.2 (${}^2J(^{119}\text{Sn-CH}_2) = 116 \text{ Hz}$).

Anal. Calcd for $\text{C}_{15}\text{H}_{22}\text{Cl}_2\text{N}_2\text{Sn}_2\cdot 2\text{CH}_2\text{Cl}_2$: C, 28.82; H, 3.70. Found: C, 28.91; H, 3.73.

Recrystallization from benzene- CCl_4 instead of CH_2Cl_2 yielded the complex free of CH_2Cl_2 (66.5-68 $^\circ\text{C}$). (Its structure was not determined by X-ray diffraction.)

With Pyrazine. To 1.0 g (2.36 mmol) of pyrazine in 10 mL of benzene was added 0.416 g (5.20 mmol) of the stannylmethane. This yielded 82% of complex **5**: mp 121-123 $^\circ\text{C}$; ${}^1\text{H NMR}$ ($\text{C}_2\text{H}_5\text{Cl}_2$) δ 0.77 (s, Sn-CH_3 , ${}^2J(^{119}\text{Sn-C-H}) = 61 \text{ Hz}$), 0.93 (s, Sn-CH_2 , ${}^2J = 61.5 \text{ Hz}$).

Anal. Calcd for $\text{C}_{14}\text{H}_{32}\text{N}_2\text{Cl}_4\text{Sn}_4$: C, 19.89; H, 3.77. Found: C, 20.11; H, 3.95.

Preparation of Complexes with Bis(dichloromethylstannyl)methane. With Pyrazine. To a solution of 1.09 g (2.36 mmol) of the stannylmethane in 10 mL of benzene was added 0.416 g (5.20 mmol) of pyrazine. Concentration yielded colorless crystals of **6**: 1.01 g (85%); mp 163-165 $^\circ\text{C}$; ${}^1\text{H NMR}$ (acetone- d_6) δ 1.33 (${}^2J(^{119}\text{Sn-CH}_3) = 90 \text{ Hz}$), 1.8 (${}^2J(^{119}\text{Sn-CH}_2) = 92 \text{ Hz}$).

Anal. Calcd for $\text{C}_7\text{H}_{12}\text{N}_2\text{Cl}_4\text{Sn}_2$: C, 16.70; H, 2.40. Found: C, 16.67; H, 2.27.

With Bipyridyl. Using the same molar quantities of the stannylmethane and bipyridyl as above led to the formation of an oil that crystallized; yielding 0.97 g (38%) of **7**, mp 220-221 $^\circ\text{C}$.

Anal. Calcd for $\text{C}_{13}\text{H}_{16}\text{Cl}_4\text{N}_2\text{Sn}_2$: C, 26.95; H, 2.78. Found: C, 27.50; H, 2.84.

With Pyridazine. To 10 mL of benzene were added 1.0 g (2.36 mmol) of the stannylmethane and 0.414 g (5.17 mmol) of pyridazine, and the mixture was warmed, whereupon an oil separated. After being left standing in the refrigerator overnight, the oil had crystallized, yielding 1.07 g (90%) of complex **3**: mp 193-194 $^\circ\text{C}$; ${}^1\text{H NMR}$ (acetone- d_6) δ 1.33 (${}^2J(^{119}\text{Sn-CH}_3) = 91 \text{ Hz}$), 1.96 (${}^2J(^{119}\text{Sn-CH}_2) = 100 \text{ Hz}$).

Anal. Calcd for $\text{C}_{11}\text{H}_{16}\text{Cl}_4\text{N}_4\text{Sn}_2$: C, 22.64; H, 2.76. Found: C, 22.33; H, 2.91.

With Pyrazole. Into a 50-mL round-bottom flask were placed 2.0 g (5.23 mmol) of the stannylmethane, 0.71 g (10.46 mmol) of pyrazole, and 20 mL of methylene chloride. The solvent was rotary-evaporated, and the residue was crystallized from hexanes to afford 2.0 g (3.85 mmol, 74%) of **4**: mp 69-70 $^\circ\text{C}$; ${}^1\text{H NMR}$ (CDCl_3) δ 0.93 (s, 12 H, ${}^2J(^{119}\text{Sn-C-H}) = 67.0 \text{ Hz}$, $-\text{SnMe}_2\text{Cl}$), 0.95 (s, 2 H, $-\text{CH}_2\text{SnMe}_2\text{Cl}$), 6.39 (t, 2 H, $-\text{NCH}=\text{CHCH}-$), 7.46 (d, 4 H, $-\text{NCH}=\text{CHCH}=\text{N}-$).

The two-bond coupling constants for the methylene protons to tins in the complex were not resolved. The solution of the complex in CDCl_3 , after treatment with aqueous HCl, showed the following ${}^1\text{H NMR}$ parameters for 1,1-bis(chlorodimethylstannyl)methane: ${}^1\text{H NMR}$ (CDCl_3) δ 0.76 (s, 12 H, ${}^2J(^{119}\text{Sn-C-H}) = 59.0 \text{ Hz}$, $-\text{SnMe}_2\text{Cl}$), 0.91 (s, 2 H, ${}^2J(^{119}\text{Sn-C-H}) = 59.0 \text{ Hz}$, $-\text{CH}_2\text{SnMe}_2\text{Cl}$) [lit.¹ ${}^1\text{H NMR}$ (CH_2Cl_2) δ 0.78 (s, 12 H, ${}^2J(^{119}\text{Sn-C-H}) = 61.0 \text{ Hz}$, $-\text{SnMe}_2\text{Cl}$), 0.93 (s, 2 H, ${}^2J(^{119}\text{Sn-C-H}) = 61.0 \text{ Hz}$, $-\text{CH}_2\text{SnMe}_2\text{Cl}$)].

Anal. Calcd for $\text{C}_{11}\text{H}_{22}\text{Cl}_2\text{N}_2\text{Sn}_2$: C, 25.48; H, 4.28; N, 10.80. Found: C, 25.76; H, 4.10; N, 10.67.

X-ray Crystallography. The details of the crystal data, data collection methods, and refinement procedures are given in Table III. Full details of the crystallographic methodologies may be found in ref 7.

Acknowledgment. We are grateful for support of this research by the National Science Foundation (Grant CHE

(7) Bruce, A.; Corbin, J. L.; Dahlstrom, P. L.; Hyde, J. R.; Minelli, M.; Stiefel, E. I.; Spence, J. T.; Zubieta, J. *Inorg. Chem.* **1982**, *21*, 917.

8318205) and by the National Institutes of Health (Grant GM 22566) for purchase of the diffractometer. Acknowledgement is also made to the donors of the Petroleum Research Fund, administered by the American Chemical Society, for partial support.

Registry No. 1, 106710-07-0; 2, 106710-08-1; 3, 106680-50-6; 4, 106680-51-7; 5, 106680-52-8; 6, 106680-49-3; 7, 106680-53-9; $(\text{CH}_3)_2\text{ClSnCH}_2\text{SnCl}(\text{CH}_3)_2$, 83135-39-1; $\text{CH}_3\text{Cl}_2\text{SnCH}_2\text{SnCl}_2\text{CH}_3$,

79992-66-8; $(\text{CH}_3)_2\text{Cl}(\text{bpy})\text{Sn}(\text{CH}_3)\text{SnCl}(\text{CH}_3)_2$, 106680-54-0; pyridine, 110-86-1; pyridazine, 289-80-5; pyrazole, 288-13-1; pyrazine, 290-37-9; bipyridine, 37275-48-2.

Supplementary Material Available: Tables of anisotropic thermal parameters and calculated hydrogen atom positions (14 pages); tables of observed and calculated structure factors (54 pages). Ordering information is given on any current masthead page.

The Making and Breaking of C-H Bonds on a Metal Cluster Framework. Analysis of the Tautomerization and Deprotonation of $\text{Fe}_3(\text{CO})_9\text{CH}_4$ Leading to the Interconversion of FeHFe and CHFe Interactions

Tamal K. Dutta, Jose C. Vites, Grant B. Jacobsen, and Thomas P. Fehlner*

Department of Chemistry, University of Notre Dame, Notre Dame, Indiana 46556

Received April 22, 1986

The hydrocarbyl cluster having the composition $\text{Fe}_3(\text{CO})_9\text{CH}_4$ (I) is shown to exist in solution as a mixture of three tautomers: $(\mu\text{-H})_3\text{Fe}_3(\text{CO})_9(\mu_3\text{-CH})$, A; $(\mu\text{-H})_2\text{Fe}_3(\text{CO})_9(\mu_3\text{-HCH})$, B; $(\mu\text{-H})\text{Fe}_3(\text{CO})_9(\mu_3\text{-H}_2\text{CH})$, C. Deprotonation of I yields the anion $[(\mu\text{-H})\text{Fe}_3(\text{CO})_9(\mu_3\text{-HCH})]^-$. Protonation of this anion is kinetically controlled, leading exclusively to C at low temperature. Rearrangement to the equilibrium distribution of tautomers occurs at higher temperatures. Aspects of the nature of the hydrocarbon-triiron interaction in the three tautomers are revealed by analyses of deuterium isotope effects and comparison of ^{13}C -H coupling constants. The latter suggests decreasing s character of the capping carbon atom in going from A to C. All these data show that the three different distributions of endo hydrogens on the capped trimetal framework are of nearly equal energy and that the interconversion of FeHC and FeHFe interactions is a facile process for this cluster system.

Besides intrinsic curiosity concerning a new class of compounds, one of the major driving forces behind the rapid development of transition-metal cluster chemistry has been the metal cluster-metal surface analogy with its relevance to chemical catalysis.¹ If the latter is to be fully meaningful, the intra- and intermolecular reactivity of the pertinent cluster models must be understood. The myriad of known cluster structures has now been rationalized in several elegant ways² with this topological understanding being supplemented by studies on the electronic properties of clusters.³ However, predictions of reactivity based on generalizations derived from stable structures suffer from the fact that a reaction path observed may reflect the high reactivity of a minor isomer rather than that of the most stable (and structurally characterized) reactant.⁴ Further, relative reactivity depends on small energy differences; i.e., small perturbations can induce large changes in rates. Indeed, the sequence of reactions occurring on a catalyst is driven by small perturbations between states of nearly equal energy. Hence, if one wants to model catalytic re-

activity with cluster chemistry, small barrier processes must be understood.

In the following, we present an investigation of the most stable positions, mobilities, and Brønsted acidities of the three endo cluster hydrogens of the geometrically simple cluster $\text{Fe}_3(\text{CO})_9\text{CH}_4$ (I).⁵ This cluster system demonstrates tautomerism involving reversible formation of CHFe interactions from FeHFe interactions, sensitivity of hydrogen arrangement to cluster charge (number of endo protons), and kinetic control of the protonation of the anionic cluster $[\text{Fe}_3(\text{CO})_9\text{CH}_3]^-$. Formally, the results constitute a demonstration of facile intramolecular formation and destruction of CH interactions in a metal cluster. Although a substantial number of mononuclear and polynuclear metal complexes containing CHM interactions have been identified,⁶ equilibria in which a CHM interaction is reversibly formed from a MHM interaction are not as common.⁷⁻⁹ Hence, our analysis is pertinent

(5) A preliminary report has appeared: Vites, J. C.; Jacobsen, G.; Dutta, T. K.; Fehlner, T. P. *J. Am. Chem. Soc.* 1985, 107, 5563.

(6) Brookhart, M.; Green, M. L. H. *J. Organomet. Chem.* 1983, 250, 395. Crabtree, R. H. *Chem. Rev.* 1985, 85, 245.

(7) Shapley and co-workers demonstrated that the equilibrium, $(\mu\text{-H})\text{Os}_3(\text{CO})_{10}(\mu\text{-HCH}_2) = (\mu\text{-H})_2\text{Os}_3(\text{CO})_{10}(\mu\text{-CH}_2)$, involves the interconversion of a CHOs interaction and an OsHOs interaction. Calvert, R. B.; Shapley, J. R. *J. Am. Chem. Soc.* 1977, 99, 5225. Calvert, R. B.; Shapley, J. R.; Schultz, A. J.; Williams, J. M.; Suib, S. L.; Stucky, G. D. *J. Am. Chem. Soc.* 1978, 100, 6240. Calvert, R. B.; Shapley, J. R. *Ibid.* 1978, 100, 7726. Recently Lewis and co-workers have reported the equilibrium $(\mu\text{-H})\text{Ru}_4(\text{CO})_{12}\text{CH} = (\mu\text{-H})_2\text{Ru}_4(\text{CO})_{12}\text{C}$. Cowie, A. G.; Johnson, B. F. G.; Lewis, J.; Raithby, P. R. *J. Organomet. Chem.* 1986, 306, C63.

(1) See for example: Muetterties, E. L. *Chem. Soc. Rev.* 1982, 11, 283.
(2) See: Wade, K. *Adv. Inorg. Chem. Radiochem.* 1976, 18, 1. Mingos, D. M. P. *Chem. Soc. Rev.* 1986, 15, 31 and references therein.

(3) See for example: Hall, M. B. In *Organometallic Chemistry*; Shapiro, B. L., Ed.; Texas A&M Press: College Station, TX, 1983; p 334. Root, D. R.; Blevins, C. H.; Lichtenberger, D. L.; Sattelberger, A. P.; Walton, R. A. *J. Am. Chem. Soc.* 1986, 108, 953. Barreto, R. D.; Fehlner, T. P.; Hsu, L.-Y.; Jan, D.-Y.; Shore, S. G. *Inorg. Chem.* 1986, 25, 3572.

(4) Kochi goes so far to suggest that if a compound obeys the 18-electron rule, it will not be an intermediate in a system. Kochi, J. K. *J. Organomet. Chem.* 1986, 300, 139.